were Grade 2. The CD45 labeling indices for Grade 1 and 2 tumors were 7.4 ± 19.7% and 4.7 ± 11.1% (p=0.47). The Ki-67+/CD45+ labeling indices for Grade 1 and 2 tumors were 0.0029 ± 0.10% and 0.60 ± 3.6% (p=0.45).
Conclusions: These results suggest that tumor-infiltrating lymphocytes did not affect the Ki-67 labeling index in this series of PanNETs, and will require validation with a larger patient population.

1802 MicroRNAs as Diagnostic Markers for Pancreatic Ductal Adenocarcinoma and Pancreatic Intraepithelial Neoplasm

Y Xue, AN Abou Tayoun, KM Abo, JM Pipas, SR Gordon, TB Gardner, RJ Barth, AA Suriawinata, GJ Tsongalis. Dartmouth-Hitchcock Medical Center, Lebanon, NH.
Background: Since the discovery of small non-coding RNAs, the analysis of microRNA (miRNA) expression patterns in human cancer have provided new insights into cancer biology. Evidence suggests that deregulated miRNA expression is associated with pancreatic cancer development. In this study, we analyzed the expression of several miRNAs in different types of pancreatic disease to determine if miRNAs expression could aid the diagnosis of pancreatic ductal adenocarcinoma (PDAC) and its precursor – pancreatic intraepithelial neoplasm (PanIN).
Design: Resection specimens containing PDAC (n=16), paired pancreatic tissue with negative margin in each case (n=16), chronic pancreatitis (n= 4), normal pancreatic parenchyma (n=5), PanIN (n=5) with different grade of dysplasia (I to III) were selected from our department archive between 2004 and 2011. These formalin-fixed paraffin embedded tissue blocks were evaluated for miR-148a, miR-196 and miR-217 expression by quantitative reverse transcription polymerase chain reaction.
Results: Our data show that miR-148a and miR-217 expression levels were significantly down-regulated in PanIN and PDAC compared to the normal pancreatic parenchyma. Comparison of these miRNA levels between the neoplastic lesions and chronic pancreatitis showed that miR-148a ($P < 0.05$) and miR-217 levels ($P < 0.0001$) were much lower in PDAC. Dramatic reduction of expression levels in PDAC was further confirmed by comparing their levels in PDAC and paired controls with negative margin which predominantly consists of chronic pancreatitis. In addition, we observed that miR-148a levels were much lower in PanIN than in chronic pancreatitis ($P < 0.05$). MiR-217 expression level also decreased, although to a lesser extent, in PanIN compared to in chronic pancreatitis ($P = 0.09$). In contrast, the level of miR-196 expression was significantly overexpressed in PanIN ($P<0.0001$) and PDAC ($P<0.0001$) compared to the non-neoplastic pancreatic parenchyma. Interestingly, the degree of deregulation of all three miRNA markers is much higher in PanIN II-III compared to that in PanIN I.
Conclusions: Our study demonstrates that miR-148a, miR-217 and miR-196a are significantly deregulated in pancreatic ductal adenocarcinoma, including in the early stage of the pancreatic ductal adenocarcinoma. Thus, these markers can be potentially used as diagnostic markers to distinguish pancreatic ductal adenocarcinoma and its precursor from benign lesions.

1803 Molecular Comparison between Intraductal Tubulopapillary Neoplasms and Intraductal Tubular Adenomas of the Pancreas Indicates Their Distinctive Nature

H Yamaguchi, M Shimizu, Y Kuboki, T Furukawa. Saitama International Medical Center, Saitama Medical University, Hidaka, Japan; Tokyo Women's Medical University, Tokyo, Japan.
Background: Intraductal tubulopapillary neoplasm (ITPN) is composed of tubulopapillary masses with high-grade atypia in the pancreatic duct. Intraductal tubular adenoma (ITA) is composed of tubular glands mimicking pyloric glands with low-grade atypia. Some may consider that ITA could be a benign counter part of ITPN, however, whether ITPN and ITA are distinctive or not is not fully assessed. In this study, we compared molecular features between ITPNs and ITAs to know their distinct or similar nature.
Design: Formalin-fixed, paraffin-embedded tissues of 14 ITPNs and 15 ITAs were investigated in this study. Foci of tumor and normal tissues were dissected separately from serial sections under microscopic guidance. Genomic DNA was extracted and somatic mutations in exons 10 and 21 of *PIK3CA*, exons 8 and 9 of *GNAS*, exons 2 and 3 of *KRAS,* and exon 15 of *BRAF* were analyzed.
Results: Somatic mutations in *PIK3CA* were found in 3 of 14 ITPNs (21.4%) but not in any of ITAs ($P = 0.0996$; Fisher exact test). In contrast, mutations in *GNAS* were found in none of the ITPNs but were found in 9 of 15 ITAs (60.0%) ($P < 0.001$; Fisher exact test). Mutations in *KRAS* were detected in 1 of 14 ITPNs (7.1%) and 12 of 15 ITAs (80.0%) ($P<0.001$; Fisher exact test). *BRAF* mutation was found in 1 ITPNs but none of ITAs.
Conclusions: These results clearly indicate that ITPNs and ITAs are molecularly distinctive from each other, which suggests that ITPNs do not evolve from ITAs. Furthermore, the molecular features of ITAs were similar to those reported in IPMNs, i.e., prevailed mutations in *GNAS* and *KRAS*, which is consistent with the renewed (2010) World Health Organization classification system for intraductal neoplasms of the pancreas that describes that intraductal neoplasms are classified into IPMNs and ITPNs, and ITA is a variant of IPMNs.

1804 Inconclusive Cytology and Non-Contributory Cyst Fluid Tumor Marker Analysis of Pancreatic Cystic Lesion: Is It the End of the Story?

M Zhang, M Carrozza, Y Huang. Temple University Hospital, Philadelphia, PA.
Background: Pancreatic cystic lesions constitute a broad spectrum of entities ranging from non-mucinous to mucinous and benign to malignant cysts. Endoscopic ultrasound -guided fine needle aspiration (EUS-FNA) cytology is routinely utilized for pre-operative diagnosis. Cyst fluid obtained from EUS-FNA is commonly submitted for chemical analysis of tumor markers to aid in the diagnosis. However, the value of cytologic interpretation is frequently limited by low cellularity of aspirated fluid and the reliability of cyst fluid tumor marker is variable. Recently, molecular tests of cyst fluid have been applied and show high specificity in the differentiation of the pancreatic cystic lesions. In this study, we investigated the usefulness of molecular analysis of pancreatic cyst fluid in the setting of inconclusive cytology and non-contributory tumor markers test.
Design: We retrospectively reviewed pancreatic cystic lesions with EUS-FNA cytology, cyst fluid tumor markers (CEA and amylase) and molecular tests (K-ras mutation and loss of heterozygocity) from 2009-2011. The inconclusive cytology diagnosis was defined as "non-diagnostic" or "atypical cytology". Non-contributory cyst fluid chemical analysis includes 2 situations: 1) amylase<250U/L and CEA <192 ng/ml or 2) amylase >250 U/L and CEA >192ng/ml. The molecular tests and the histopathologic results of the resection specimens were analyzed.
Results: The cohort consists of 32 pancreatic cyst EUS-FNA cytology cases, which shows 20 cases (62.5%) with non-diagnostic (34.4%) or atypical (28.1%) cytology. Among the 20 cases, non-contributory tumor marker analysis was found in 11 cases (55%). The molecular analysis shows K-ras mutation or loss of heterozygocity in 5 out of 11 cases (45%), which also indicates a mucinous cystic neoplasm with potential for neoplastic progression. Interestingly, 3 out of 4 pancreatic cyst resection specimens showed pancreatic intraepithelial neoplasias (PanIN)-1A or 1B with benign molecular features; while elevated cystic fluid CEA and amylase were identified in all the cases with PanIN-1A and 1B.
Conclusions: Inconclusive pancreatic cyst cytology and non-contributory cystic fluid tumor markers were frequently encountered, making accurate diagnosis challenging. Our study indicates that cyst fluid molecular tests for K-ras mutation and allelic imbalance provide extra information and may help with the diagnosis and clinical management. Our novel finding is that PanIN-1A and 1B might be related to both elevated cyst fluid CEA and amylase without K-ras mutation.

Pan-genomic/Pan-proteomic approaches to Cancer

1805 Characterization of Cell Type Specific miRNA Profiles and Application to miRNA Profiles Derived from Tissues

AS Baras, M McCall, T Cornish, M Halushka. Johns Hopkins Hospital, Baltimore, MD; University of Rochester, Rochester, NY.
Background: MicroRNAs (miRNAs) are highly conserved RNAs that serve as master regulators of gene expression. They are exciting biomarkers and therapeutic targets. Studies have found altered expression of miRNAs in tissue disease states; however, the interpretation of these studies may be fundamentally flawed because the changing cellular composition of tissues in disease states is not adequately accounted for. Techniques to control for this source of variability should increase the relevance of changes in miRNA species identified in profiling studies of diseased tissue.
Design: Our approach characterizes both factors that can affect miRNA expression levels: altered cellular composition of tissue and disease specific expression changes. We have utilized miRNA expression profiles from a panel of cell types to deconvolute observed miRNA profiles generated from various tissues. We have then explored the impact of this two factor analysis via a modeling study of ulcerative colitis.
Results: We utilized publicly available data from 16 cell types including inflammatory, endothelial, stromal, and epithelial cells to predict the cellular composition and model the observed expression of the miRNA expression profile from 4 tissues (Fig. 1A). The predicted cellular compositions are consistent with the expected composition of these tissues and the modeled miRNA levels are highly correlated to the observed signals. We next performed a modeling experiment of ulcerative colitis using image analysis to predict cellular ratio changes (Fig. 1B). We generated hypothetical miRNA profiling data of normal colon and ulcerative colitis in which we manually altered only 3 miRNAs at the cell level – potential disease specific changes. We then analyzed the data via routine univariate hypothesis testing with and without correction for changes in tissue composition. Without tissue composition correction, most miRNAs identified are false positives (Fig. 1C).

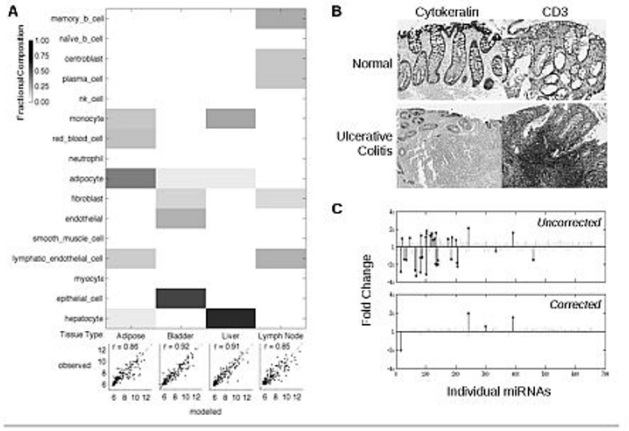

Figure 1A. Reconstruction of adipose, bladder, liver, and lymph node tissues from individual cell-type miRNA profiles. A strong agreement between the modeled data and the observed tissue miRNA expression is present and the biologically expected cell types are correctly identified in these tissues.

Figure 1B. Normal colon and ulcerative colitis with the change in cellular composition highlighted by cytokeratin (epithelial cells) and CD3 (inflammatory cells) immunohistochemical staining
Figure 1C. Fold changes for the miRNA species with and without correction for cellular composition. Astericks mark significant changes after multiple testing correction (false discovery rate < 0.05).

Conclusions: The findings highlight the importance of understanding the cellular contribution of miRNAs to tissue expression data and controlling for changes in cellular composition in disease analysis.

1806 MEK Inhibition Induces Differential Mechanisms of Resistance in Thyroid and Melanoma BRAF^{V600E} Cell Lines

ER Dorris, M Alhashemi, R Dunne, P Smyth, JJ O'Leary, O Sheils. Trinity College Dublin, Dublin, Ireland.

Background: Oncogenic mutations in BRAF are common in melanoma and thyroid carcinoma and drive constitutive activation of the MAPK (RAS/RAF/MEK/ERK) pathway. Molecularly targeted therapies of this pathway improves survival compared to chemotherapy; however, responses tend to be short-lived as resistance invariably occurs. In this study the molecular pathology of resistance to therapeutic MEK inhibition in BRAF^{V600E} melanoma and thyroid cells was investigated.

Design: Cell line models of melanoma and thyroid carcinoma, +/- BRAF^{V600E} activating mutation, were treated with the MEK inhibitor PD0325901 and resistant cells were harvested. Resistant and treatment naive samples were assayed for relative gene and protein expression of key members of the MAPK pathway and stemness-markers. Global microRNA expression profiling of naive and resistant cells was performed via next generation sequencing.

Results: Members of the *MIR302/373/374/520* family of embryonic stem cell specific cell cycle regulating (ESCC) microRNAs were identified as differentially expressed between resistant BRAF^{V600E} melanoma and thyroid cell lines. Upregulated expression of gene and protein stemness markers, upregulated expression of MAPK pathway genes and downregulation of the ESCC *MIR302* cluster in BRAF^{V600E} melanoma indicated an increased stem-like phenotype in resistant BRAF^{V600E} melanoma. Conversely, downregulated expression of gene and protein stemness markers, downregulated expression of MAPK pathway genes, upregulation of the ESCC *MIR520* cluster, reeexpression of cell surface receptors, and induced differentiation-associated morphology in resistant BRAF^{V600E} indicate a differentiated phenotype associated with MEK inhibitor resistance in BRAF^{V600E} thyroid cells.

Conclusions: The differential patterns of resistance observed between BRAF^{V600E} melanoma and thyroid cell lines may reflect tissue type or *de novo* differentiation, but could have significant impact on the response of primary and metastatic cells to MEK inhibitor treatment. This study provides a basis for the investigation of the cellular differentiation/self-renewal access and its role in resistance to MEK inhibition.

1807 T-Cell Clonality Testing by Next Generation Sequencing: A Comparison of Benchtop Sequencing Platforms

E Duncavage, J Schumacher, P Szankasi, T Kelley. Washington University in St Louis, St. Louis, MO; ARUP Laboratories, Salt Lake City, UT; University of Utah, Salt Lake CIty, UT.

Background: Next-generation sequencing (NGS) is rapidly becoming a standard laboratory technique in molecular onclology, in part due to newer, inexpensive platforms such as the Ion Torrent (Life Technology) and MiSeq (Illumina). One potential application of NGS is the analysis of the T-cell receptor (TCR) gamma repertoire in patients with suspected T-cell malignancies. Current methodologies rely on capillary electrophoresis (CE) of amplified TCR gamma sequences, with clonality determined by peak height over the polyclonal background. This method is not sufficiently sensitive for minimal residual disease testing, and is often confounded by apparent oligoclonal populations. Here we describe a study designed to compare sequencing the TCR gamma repertoire on the Ion Torrent versus the MiSeq.

Design: PCR primers were designed to target TCR V-gamma 2 through V-gamma 11+J gamma rearrangements in a single multiplex reaction. Genomic DNA (400 ng) from six patient samples was subjected to PCR amplification. Amplicons were purified and 500ng indexed for Ion Torrent and MiSeq analysis. Indexed libraries were sequenced in pairs using the Ion Torrent 314 chip or as a single pool on the MiSeq using 2x150bp reads. Contigs were reconstructed from the paired-end MiSeq reads. Data were analyzed by first identifying the most common reads and then mapping reads to a database of TCR sequences. T-cell clonality was established by examining the distribution of TCR sequences.

Results: Data from both the Ion Torrent and MiSeq correctly identified 2/2 cases called polyclonal by CE and 2/2 cases called clonal by CE. In the 2 cases called oligoclonal by CE, both the MiSeq and the Ion Torrent identified the same small clonal populations, as determined by the V region sequence. While the overall results of the MiSeq and Ion Torrent were similar, the Ion Torrent produced a larger number of background sequences, which obscured analysis by PCR product size distribution.

Conclusions: T-cell clonality testing by NGS is a robust alternative to standard CE detection and provides the ability to accurately identify small populations that may be missed by CE. Further, as the exact clonal V region sequence is known, NGS methods have the potential to improve minimal residual disease detection and establish a clonal relationship between recurrent specimens.

1808 Differential MicroRNA Expression in Colorectal Cancer Patients Presenting with Synchronous Hepatic Metastases

CJ Ellermeier, K Cleveland, AS Brodsky, M Resnick. Rhode Island Hospital/Warren Alpert Medical School of Brown University, Providence, RI.

Background: MicroRNAs (miRNAs) are a class of highly conserved ~[/underline]22-nucleotide single-stranded RNAs that bind complementary sequences of messenger RNA (mRNA) and induce translation repression and/or mRNA degradation. While previous publications have described associations between specific miRNAs and colorectal cancer (CRC) metastases, there are still many aspects of RNA regulators of metastatic spread that are unexplored. We examined the differential expression of miRNAs in CRC primary tumors with synchronous liver metastases and analyzed miRNA expression correlation with patient survival.

Design: Thirty-one colorectal cancer (CRC) cases selected from the Lifespan Hospital System archives were analyzed. Portions of both colonic and liver formalin fixed paraffin embedded tissue sections were laser capture microdissected. RNA was extracted and miRNAs were then amplified using qRT-PCR. Individual miRNAs were identified using array cards with miRNA expression quantitated using qRT-PCR. Expression in primary tumors, liver metastases, and differential expression were tested for association with length of survival.

Results: 20 different miRNAs showed significant differential expression between CRC primary tumors and liver metastases. Of these 20, 6 (miR-210, miR-133b, miR-708, miR-548a-3p, miR-204, miR-618) were confirmed by quantitative PCR (paired t-test, $p<0.05$). Analysis reveals that the change in expression levels of miR-210 (mean=4.2 fold, median=2.5 fold, standard deviation=7.1) and miR-133b (mean =76.1 fold, median=0.2 fold, standard deviation=369.3) between primary and metastatic tumors are significantly associated with overall survival, with both miRNAs showing increased expression in liver metastases. Increased miR-133b and miR-210 expression in liver metastases when compared to primary CRC tumor showed a hazard ratio of 1.9 ($p=0.04$ with Cox proportional hazards model: 95% confidence levels; 1.03 to 3.7). miR-210 expression also correlates with tumor necrosis as identified by microscopic morphology.

Conclusions: This is the first study to show association of differential expression of miR-210 and decreased length of survival. While miR-133b was previously shown to be downregulated in colorectal cancers, our study shows that, despite the low absolute expression of miR-133b in both primary CRC tumor and liver metastases, a relative increase in expression in metastastic disease is associated with significantly decreased overall survival.

1809 Two New Stromal Signatures Stratify Breast Cancers with Different Prognosis

X Guo, SX Zhu, K Montgomery, M van de Rijn, RB West. Stanford University School of Medicine, Stanford, CA.

Background: Carcinoma is comprised of malignant epithelial cells and the tumor microenvironment. Although the initiation and progression of carcinoma involves the acquisition of mutations and the dysregulation of gene expression in the neoplastic epithelia cells, results over the last couple of decades has showed that the microenvironment plays an important role in the initiation, progression and metastasis of cancer. Our group previously identified stromal gene expression signatures associated with outcome differences in breast cancer using gene expression microarrays.

Design: In order to find new types of tumor stroma gene expression patterns, we have gene expression profiled 10 types of different fibrous tumors. Because these are uncommon tumors not typically fresh frozen, we used a modified RNA-seq protocol that we developed, 3'end sequencing (3SEQ), to identify different fibrous tumor specific gene expression signatures.

Results: 53 fibrous tumors representing 10 groups of benign fibrous tumors were expression profiled, and an average of 29 million reads were generated for each sample. Only the elastofibromatosis (EF) and fibromatosis of tendon sheath (FOTS) gene signatures demonstrated robust outcome results for survival in the four breast cancer datasets. The EF signature positive breast cancers (20-33%) demonstrated significantly better outcome for survival. In contrast, the FOTS signature positive breast cancers (11-35%) had a worse outcome. While the EF and FOTS signatures shared some assigned breast cancer cases with two previously identified stromal signatures (DTF fibroblast and CSF1 macrophage signatures), they were statistically independent signatures in three of the four data sets. EF+ breast cancers showed best outcome in survival independent of whether the breast cancer is DTF+ or DTF-. The EF+/DTF+ breast cancers were significantly more likely to be ER positive, PR positive, low grade, p53 wild type than EF-/DTF- breast cancers. FOTS+/CSF1- breast cancer showed the worst outcome in survival. FOTS+/CSF1+ breast cancers were significantly more likely to be ER negative, PR negative, Grade 3, p53 mutant than FOTS-/CSF1- breast cancers.

Conclusions: Over all, we defined and validated two new stromal signatures in breast cancer (EF and FOTS), which showed robust prognosis indication in breast cancer. The combined stromal signatures of EF, FOTS, DTF fibroblast, and CSF1 macrophage identifies between 74%-90% of all breast cancers.

1810 Spectrum of Non-Synonymous Mutations in Cancer Identified by Clinical Targeted Next-Generation Sequencing

IS Hagemann, H Al-Kateb, CE Cottrell, C Lockwood, TT Nguyen, D Spencer, A Bredemeyer, R Head, S Shrivastava, R Nagarajan, K Seibert, EJ Duncavage, S Kulkarni, JD Pfeifer. Washington University, St. Louis, MO.

Background: We have implemented a clinical assay using next-generation sequencing (NGS) to analyze twenty-five genes relevant to multiple cancer types. We report findings from 155 consecutive malignancies submitted to Genomics and Pathology Services at Washington University in St. Louis (GPS@WUSTL).

Design: DNA was extracted from up to six 1 mm cores of tumor formalin-fixed, paraffin-embedded (FFPE) tissue after histopathologic review. Up to 1 µg of DNA (minimum, 0.2 µg) was subjected to library preparation using liquid-phase cRNA capture probes targeting a 300 kb region consisting of all exons of *BRAF, CTNNB1, CHIC2, CSF1R, DNMT3A, EGFR, FLT3, IDH1, IDH2, JAK2, KIT, KRAS, MAPK1, MAP2K2, MET, NPM1, NRAS, PDGFRA, PIK3CA, PTEN, PTPN11, RET, RUNX1, TP53,* and *WT1*. Libraries were sequenced using Illumina technology to obtain 101 bp or 150 bp paired-end reads. Mean depth was >5660x, and 50x coverage was achieved at >95% of positions. The analysis pipeline was validated for variant allele frequencies >10%. Variants were called, prioritized, and interpreted using a custom software package. A list of actionable variants was prepared by literature review.

Results: Of 155 cases, 79 (50%) were non-small cell lung cancer (NSCLC), 19 (12%) were pancreatic malignancies, and 15 (9.4%) were colorectal cancer, with the balance representing 22 diverse other malignancies. FFPE tissue cores yielded a median of 2.7 µg DNA (interquartile range, 1.19-5.55 µg). Sequencing identified a mean of 4.6 non-synonymous variants per case (single-nucleotide variants and indels). Of these, a mean of 2.5/case were not known polymorphisms and most likely represented somatic mutations. Somatic variants most commonly occurred in *TP53* (127/155 cases), *KRAS* (45 cases), and *EGFR* (20 cases). Sequencing identified 57 clinically actionable (i.e., predictive or prognostic) mutations in 46/155 = 30% of cases. In NSCLC, actionable mutations were present in *KRAS* codon 12 (22/78 cases), *EGFR* exon 21 (5 cases), and the *PIK3CA* helical domain (4 cases). In pancreatic cancer, there were no variants currently recognized as actionable. In colorectal cancer, actionable mutations were present in *KRAS* codon 12 or 13 (6/15 cases) or *PIK3CA* (3 cases). Average turnaround time was 29 days.

Conclusions: NGS-based diagnostics can provide clinically relevant information using readily available FFPE tissue. Actionable variants were identified in 30% of cases. Targeted therapies exist for many of these mutations, suggesting that such diagnostics have the potential to improve patient outcome.

1811 When To Use Gene Expression Profiling? A Direct Comparison with Immunohistochemistry for Diagnosing the Primary Site in Metastatic Cancer

CR Handorf, A Kulkarni, JP Grenert, LM Weiss, WM Rogers, OS Kim, FA Monzon, M Halks-Miller, GG Anderson, MG Walker, R Pillai, WD Henner. University of Tennessee College of Medicine, Memphis, TN; University of California San Francisco, San Francisco, CA; Clarient Inc., Aliso Viejo, CA; El Camino Hospital, Mountain View, CA; Advocate Good Shepherd Hospital, Barrington, IL; Baylor College of Medicine, Houston, TX; Pathwork Diagnostics, Redwood City, CA; DegreesBiosciences, San Jose, CA; WalkerBioscience, Carlsbad, CA.

Background: Pathologists commonly use a battery of immunohistochemical (IHC) stains to determine the primary site of metastatic cancers. Gene expression profiling (GEP – Pathwork Tissue of Origin Test), is an alternative method for evaluating these cases. We directly compared the accuracy of IHC and GEP and identified subgroups where GEP is most beneficial.

Design: This prospectively conducted, blinded, multicenter study compared the diagnostic accuracy of GEP and IHC in 157 formalin-fixed paraffin-embedded specimens from metastatic tumors with known on-panel primaries in order to have a gold standard to compare diagnostic accuracy. Four pathologists selected from 84 stains in two rounds to render diagnoses. Conditional logistic regression was used to compare the results from the two methods.

Results: 157 samples were evaluated by both IHC and GEP. The GEP test results were more accurate at identifying the primary site for metastatic tumors (89%) than IHC (83%) (p=0.013). GEP was substantially more accurate (94%) than IHC-based diagnoses (79%) in 51 poorly differentiated or undifferentiated samples (p=0.016). The difference was most pronounced in 33 poorly differentiated carcinomas, 91% for GEP vs. 71% for IHC (p=0.022). In samples for which pathologists rendered their final diagnosis with a single round of stains, both IHC and GEP exceeded 90% accuracy. However, when the diagnosis required a 2nd round, IHC significantly underperformed GEP (67% to 83%, P<0.001). When 6 or more first round stains were used, GEP was more accurate than IHC (88% vs. 79% respectively, p=0.012).

Conclusions: The GEP test used in this study was significantly more accurate than IHC when used to identify primary site with the most pronounced superiority observed in specimens that required a 2nd round of stains, 6 or more stains in the first round, and in poorly differentiated and undifferentiated metastatic carcinomas.

1812 Somatic Mutations Implicated in Progression from Well-Differentiated to Dedifferentiated Liposarcoma: An Exome Sequencing Approach

AE Horvai, K-Y Jen. UCSF, San Francisco, CA.

Background: The well-differentiated/dedifferentiated liposarcoma family represents the most common subtype of liposarcoma. Well-differentiated (WL) and dedifferentiated liposarcomas (DL) demonstrate amplification of chromosome subregion 12q13-q15. Preliminary data on a few liposarcoma cases have uncovered point mutations in specific genes (*HDCA1, PTPN9* and *DAZAP2*) when compared to normal tissue. However, the specific genetic changes that distinguish *between* WL and DL, which may provide insights into tumor progression, are poorly understood. Upregulation of the MAPK-AP1 signaling axis has been proposed, but the mechanism is not known. The presence of discrete lipogenic and non-lipogenic components in DL provides a unique model system to investigate mechanisms of progression. Using high throughput exome sequencing we delineated the mutations that are unique to only the nonlipogenic components of DL, but are not present in matched lipogenic components.

Design: Two DL, with confirmed 12q13-15 amplification, were selected from departmental archives. Matched normal tissue, lipogenic and nonlipogenic ("dedifferentiated") areas were separately dissected from formalin-fixed, paraffin embedded (FFPE) tissue. Each component was analyzed by whole exome sequencing using the Illumina platform achieving 86-fold average coverage. The data were filtered for known SNPs and analyzed for nonsynonymous somatic mutations and small insertions and deletions (indels).

Results: Fifty-seven genes were identified with point mutations that were present in nonlipogenic components of both DL but not in either matched lipogenic component or normal tissue. The presumed functions of mutated genes include signal transduction (*RASSF1*), tyrosine kinase receptor (*FLT4*), cell cycle control (*UBXN11*) and fatty acid metabolism (*ACOX1*). Mutations in the *MAPK* or *AP1* families of genes were not observed. Indels of 30 and 33 genes, respectively, were identified in the nonlipogenic components, but none were common to both tumors.

Conclusions: Whole exome sequencing from FFPE tissue is a useful tool in the discovery phase to identify genes that drive tumorigenesis and progression. This study identifies novel somatic mutations in DL, a subset of which are specific to the nonlipogenic component. That many such mutations affect genes involved in cell proliferation suggests oncogenic potential in DL and are good candidates for further study.

1813 Use of Targeted Deep Sequencing To Analyze the Genomic Similarities of Concurrent Acute Myeloid Leukemia in the Peripheral Blood and Bone Marrow

JM Klco, DH Spencer, C Miller, T Lamprecht, RS Fulton, L Ding, RK Wilson, TJ Ley. Washington University School of Medicine, St Louis, MO; Washington University, St Louis, MO.

Background: Acute myeloid leukemia (AML) is a clonally heterogeneous disease composed of a founding clone with hundreds of single nucleotide variants (SNVs) and frequently multiple subclones derived from the founding clone that contain additional variants. Recently it has been demonstrated that significant spatial heterogeneity exists within solid tumors. Whether AML demonstrates similar spatial heterogeneity (i.e. disease in the bone marrow versus peripheral blood), both at the level of specific subclones and individual SNVs, has not been evaluated, yet is critically important in the context of clinical testing.

Design: We identified 4 oligoclonal (3-4 clones) *de novo* bone marrow AML samples previously characterized by whole genome sequencing that also had significant peripheral blood involvement (69.2% blasts, mean). Using custom capture arrays containing all the known variants in these genomes (640.3 SNVs, mean) followed by deep sequencing on the Illumina platform, we analyzed the similarities in the variant allele frequencies (VAFs) in concurrent leukemia from the bone marrow and peripheral blood.

Results: We obtained deep coverage (569 x coverage, mean) of all the SNVs and exonic insertions/deletions identified in the 4 AML genomes, allowing us to digitally report VAFs and identify clusters of variants with similar VAFs, representing distinct subclones. When corrected for blast counts, the founding clones in each case were present at indistinguishable VAFs in the peripheral blood and bone marrow; the average difference in mean VAF between the founding clone in the peripheral blood and bone marrow was only 0.60% (range, 0.08-1.27%). Similar findings were seen for all the minor subclones. Analysis of individual cases demonstrated strong concordance for known AML mutations, including *DNMT3A* (BM: 52.5%; PB: 49.5%), *NPM1* (BM: 44.6%; PB: 43.6%), *IDH1* (BM: 34.4%; PB: 37.7%), and *FLT3* (BM: 38.6%; PB: 31.4%).

Conclusions: In a small cohort of AML samples we found that clonal heterogeneity and VAFs of known pathologic mutations are similar in the bone marrow and peripheral blood at the time of diagnosis. These studies are currently being expanded to a larger cohort of AML samples and suggest that peripheral blood will be a suitable surrogate for clinical testing using next generation sequencing technologies for most AML cases.

1814 Next Generation Sequencing in Clinical Environment for Cancer Therapy

B Lee, Y-L Choi, HY Park, YH Ko. Samsung Medical Centre, Sungkyunkwan University School of Medicine, Seoul, Korea.

Background: Clinical practice for targeted therapy requires rapid approaches that are compatible with small input amounts of nucleic acids derived from challenging samples including formalin-fixed paraffin-embedded (FFPE) tissues. Furthermore, the number of targetable genes is increasing and multiplex testing with small amount of sample is required. By overcoming known barriers of multiplex PCR, the Ion AmpliSeqTM

technology introduces a groundbreaking workflow enabling the rapid sequencing of hundreds of known mutations with low-frequency allele detection. The Ion AmpliSeq Cancer Panel consists of 190 amplicons and surveys 790 known cosmic mutations in approximately 20 kb of sequence from 46 genes including EGFR, KRAS and BRAF. This kit is ideally suited for both fresh and FFPE samples, requiring only 10ng of DNA per reaction.

Design: Library preparation was performed according to the manufacturer's protocol. Library constructions of the amplicons and subsequent enrichment of the sequencing beads were performed using the OneTouch system. Sequencing was done on the 316 chip with 10 megabases capacity using the Ion Torrent PGM (Life Technologies) as per the manufacturer's protocol. Data analysis, including alignment to human reference genome and base calling, was done using built-in software. We tested 60 solid cancers including bladder, gastric, breast, colon, kidney, lung and pancreatic cancer using fresh or FFPE samples.

Results: The turn-around-time was about 1 week from sample preparation to final analyzed report. Some of results were validated by Sanger sequencing. False positive calling by homopolymer deletion was identified. Mean read coverage of amplicons at the known cosmic hotspot mutation sites was calculated, and we noticed that each amplicon showed various read coverage (5X to ~[/underline]11,000X).Many amplicons of FFPE had slightly less coverage than fresh samples. Most cases showed one or two mutation among 46 genes, most common gene are as follows; TP53, KRAS, and PIK3CA.

Conclusions: The Ion AmpliSeq Cancer Panel contains most actionable genes that have been tested in clinical lab with reasonable turn-around time and high accuracy. Furthermore, this is applied to small samples of FFPE which is most common sample type in clinical environment.

1815 Abstract Withdrawn.

1816 Profile: Results from Multiplexed Mass Spectrometric Genotyping of 2178 Cancer Patients

NI Lindeman, LE MacConaill, E Garcia, FC Kuo, JA Longtine, WC Hahn, PW Kantoff, BJ Rollins. Harvard Medical School, Boston, MA; Brigham and Women's Hospital, Boston, MA; Mt. Sinai Hospital, New York City, NY; Dana-Farber Cancer Institute, Boston, MA.

Background: The Profile initiative is a joint venture between the Brigham and Women's Hospital (BWH) and the Dana-Farber Cancer Institute (DFCI) to perform high throughput molecular analysis of samples from all new cancer patients. The initial assay was designed to detect sequence alterations in known oncogenes and tumor suppressor genes, to identify patients suitable for clinical trials and to foment new biological investigations.

Design: Test requisitions were submitted for all new patients who provided informed consent. Tested samples included fresh and formalin-fixed paraffin-embedded tissues, marrow, and blood. Analysis was not performed on samples without invasive cancer, <50% malignant cells, <5 mm in greatest dimension, or samples that were decalcified. 471 mutations in 41 genes were assessed by a PCR-single nucleotide extension-mass spectrometry assay (Sequenom). Mutations were classified into three interpretive categories: Tiers 1 (standard-of-care), 2 (useful for clinical trials), and 3 (unknown significance).

Results: Over one year, requisitions were received from 8624 patients who consented to testing. Of these, 3309 (38%) had adequate samples within the BWH pathology department; 2258 (27%) of samples were archived at the patients' primary institutions and unavailable for analysis, and 3057 (35%) were insufficient. Tests were completed on 2178 samples, of which 879 (40%) had at least one mutation and 215 (10%) had multiple mutations. 25% of mutations were in either Tier 1 or 2. The highest mutation rates were seen in GI (64%), GYN (59%), and Endocrine (59%) cancers, whie the lowest (~[/underline]30%) were seen in GU, Head/Neck and sarcomas. The most frequent genes altered were *KRAS* (18%), *PIK3CA* (16%), and *TP53* (10%). Of the targetable oncogenes, *PIK3CA* was seen in the widest range of cancer types. 10% of samples with *PIK3CA* mutations had another mutation.

Conclusions: Multiplexed genotyping of all new cancer patients' samples in a referral cancer center is feasible. By genotyping 471 mutations in 41 cancer-related genes, at least one mutation was found in ~[/underline]40% of samples; of these ~[/underline]25% were relevant for either standard therapy or clinical trial agents. Transition to next generation sequencing will expand testing to a greater number of samples and gene targets.

1817 Genomic Landscape of Bladder Cancer Development from Incipient Field Effects to Invasive Disease

T Majewski, J Bondaruk, W Choi, S Lee, W Chung, K Baggerly, C Dinney, HB Grossman, J-P Issa, D McConkey, S Scherer, B Czerniak. UT MD Anderson Cancer Center, Houston, TX; Texas Human Genome Sequencing Center, Baylor College of Medicine, Houston, TX; Temple University School of Medicine, Philadelphia, PA.

Background: We are pursuing a unique strategy to identify early events in bladder cancer development by the analysis of somatic changes in tissues from resected bladder and characterized pathologically as transitional cell carcinoma and then extending this analysis outward into precursor intraurothelial lesions and normal tissue.

Design: We used the whole-organ histologic and genetic mapping strategy coupled with next generation whole exome sequencing using a combination of NimbleGen whole exome capture with Illumina HiSeq 2000 exome sequencing (20x coverage) complemented with custom genotyping using Illumina HumanOmni2.5_8 chips and whole genome methylation analyses to define the molecular alterations that were associated with the progression of muscle-invasive bladder cancer in one surgical specimen.

Results: We identified a total of 18 structurally significant mutations, three of which appeared to be clear "driver" mutations that had been annotated previously. Alterations in chromatin hyper- and hypomethylation predominated in all of the regions that contained normal-appearing urothelium or low-grade dysplasia. In total, 31 genes were hypermethylated and 26 genes were hypomethylated. Copy number alterations were numerous (n=242) in areas that contained high-grade dysplasia suggesting that genomic instability preceded the emergence of driver mutations in what ultimately emerged as the dominant tumor subclone. Chromosomal gains (n=216) vastly outnumbered losses (n=26) suggesting that genomic instability was not a random process. Finally, genomic instability increased dramatically at the transition from high-grade dysplasia to TCC.

Conclusions: Our study has important implications for understanding the "field effect" that underlies bladder cancer carcinogenesis and progression. The data strongly suggest that epigenetic (methylation-based) alterations targeting DNA repair, developmental signaling, and invasion/migration were present at the earliest stages throughout the urothelium and were most likely responsible for the genomic instability and proliferation that lays the foundation for progression to high-grade dysplasia.

1818 Methylation Patterns of Oligodendroglial Tumors

B Melendez, P Mur, M Mollejo, C Fiano, JF Garcia, A Hernandez Lain, A Rodriguez de Lope, JA Rey. Virgen de la Salud Hospital, Toledo, Spain; Xeral-Cíes Hospital, Vigo, Spain; MD Anderson International, Madrid, Spain; 12 de Octubre Hospital, Madrid, Spain; Puerta de Hierro Hospital, Madrid, Spain; La Paz Hospital, Madrid, Spain.

Background: Oligodendroglial tumors (OTs) present a variable biological behaviour depending on the presence of 1p/19q deletion and IDH mutation. Combined 1p/19q loss occurs in oligodendrogliomas and mixed oligoastrocitomas. The presence of this deletion involves better prognosis and treatment response. A prognostically favorable CpG island methylation phenotype was reported in gliomas (G-CIMP+). Recently, G-CIMP+ tumors have been associated to IDH mutations. The major goal of this study was to analyze the methylation status of the whole genome in OTs.

Design: We included 46 high and low grade OTs (34 oligodendrogliomas and 12 oligoastrocytomas), and 5 non-tumoral brain samples as controls. Whole genome methylation profiling analyses were performed (450K, Illumina). Our results were validated by using external datasources. Tumors were characterized for 1p/19q codeletion by FISH or LOH, and for IDH mutation by direct sequencing.

Results: The G-CIMP+ phenotype was strongly associated to IDH mutation and to combined 1p/19q loss, while G-CIMP- tumors did not show either IDH mutation or 1p/19q codeletion. Furthermore, G-CIMP+ tumors could be separated into two groups according to the different methylation profile: i) tumors G-CIMP+, which showed IDH mutation and 1p/19q codeletion; and ii) tumors showing an intermediate methylation profile (G-CIMP+/-), featured by IDH mutation and absence of 1p/19q codeletion. These different G-CIMP profiles did not correlate with tumoral grade or subtype. Methylation data from glioblastomas (TCGA database) showed that most of primary GBMs were G-CIMP-, while a few of them presented a G-CIMP+/- profile. Striking differences on overall survival times ($P<0.01$) were observed between G-CIMP- and either G-CIMP+ or G-CIMP+/-, which could be due to lack of good prognostic molecular features of G-CIMP- tumors. A non-significant tendency toward a better overall survival of G-CIMP+ tumors compared to G-CIMP+/- is also observed.

Conclusions: This study allowed us to classify OTs according to their methylation profiles, which were related to the IDH and 1p/19q status, but were independent of the tumoral grade or subtype. Higher levels of aberrant methylation (CIMP+) were identified in IDH mutated, 1p/19q deleted tumors. Intermediate methylation profiles were observed in IDH mutated tumors with intact 1p/19q. The G-CIMP status could have an important impact on survival.

1819 Analysis of Angiogenesis-Related Gene Expression Reveals a Profile with Prognostic Implications in Endometrioid Endometrial Carcinoma

M Mendiola, A Redondo, J de Santiago, A Hernandez, E Perez-Fernandez, M Miguel-Martin, E Diaz, J Barriuso, V Heredia, L Yebenes, J Feliu, D Hardisson. Hospital La Paz Institute for Health Research (IdiPAZ), Madrid, Spain; La Paz University Hospital, Madrid, Spain.

Background: Endometrial cancer is the most common gynecologic malignancy in developed countries but little is known about the underlying mechanisms of tumor progression. Endometrioid adenocarcinoma (EAC) is the most frequent subtype and account for more than 80% of all endometrial adenocarcinomas. EAC tend to present as low grade, early stage tumors with good outcomes, often cured with surgery alone. However, approximately 15% of women with EAC will present with advanced FIGO stage and have a shorter 5-year survival rate. Enhanced tumor angiogenesis regulates the progression of endometrioid carcinomas. We have been focused on a selected group of genes related to this process in an attempt to identify a gene expression profile useful as prognostic marker for overall survival in EAC.

Design: 61 patients with EAC were included in this study. RNAs were collected from formalin-fixed paraffin-embedded samples. Specific TaqMan Gene Expression assays for 82 genes were selected and gene expression was determined by qRT-PCR with TaqMan Low Density Arrays (Applied Biosystems). We applied a normalization factor based on the geometric mean of 8 housekeeping genes, selected by Genorm Software. A logistic regression analysis was used to build multiple models based on the combination of significant genes selected by the Akaike Information Criterion. The accuracy of the model was determined by using the receiver operating characteristics (ROC). SAS 9.1 and SPSS packages were used for statistical tests.

Results: The mean overall survival was 152 months. We generated a predictive model based on the expression of 5 angiogenesis-related genes. According to the model, patients were divided into 2 risk groups, with 85% sensibility and 72% specificity. In a multivariate analysis including clinical variables the model was independently associated with overall survival.

Conclusions: These preliminary data support the relation of the angiogenic process with the prognosis of endometrioid endometrial carcinomas. Once validated, this 5-gene expression profile could be clinically useful for stratifying patients according to the risk of tumor progression and outcome.

1820 Phosphoproteomic Analysis Identifies Deregulated Expression of Acting Signaling Networks in T Cell Lymphomas

C Murga-Zamalloa, D Rolland, Y Jeon, V Basrur, K Elenitoba-Johnson, M Lim. University of Michigan, Ann Arbor, MI.

Background: Proteins involved in actin dynamics play a key role in lymphocyte biology and have been implicated in lymphomagenesis. Actin polymerization in T-cells is tightly regulated by phosphorylation of key proteins such as WASP and CRKL. Identification of novel phosphoproteins would be critical for studying the signaling networks involved in lymphocyte biology and lymphomagenesis. In order to identify actin signaling networks which are activated in T-cell lymphomas, we carried out mass spectrometry-based proteomic analyses to identify phosphoproteins in T-cell lymphoma derived cell lines.

Design: Phosphorylated peptides of CTCL (HH, HUT78 and MAC1), ALK+ ALCL (SUPM2, SUDH1L and KARPAS 299) and NK lymphoma (NK92MI and YT) cell lines were enriched using immobilized metal affinity chromatography (IMAC) and phospho-tyrosine immunoaffinity purification and subsequently analyzed by liquid chromatography and high mass accuracy tandem mass spectrometry (LC-MS/MS). Proteins involved in actin regulation and signaling networks were identified using DAVID and STRING software, respectively. Hierarchical cluster analysis was performed with MeV software.

Results: Serine, tyrosine and threonine phosphorylated peptides from sixty one proteins involved in the regulation of the actin cytoskeleton were identified. Phosphorylation motif analysis indicated that many of these peptides are targets of GSK-3, GRK-1 and Casein kinase 1. Proteins associated with lymphomagenesis such as TWF1, CRKL, WASP and a role in migration (paxillin and zyxin) were identified to be differentially phosphorylated. A subset of proteins was specific to distinct disease categories; GRLF1 in NK lymphoma; CASL in CTCL and VASP in ALCL. Interestingly, hierarchical clustering using the sixty one proteins grouped the ALK+ ALCL cell lines distinct from the others. Protein network analysis revealed that WASP and NCK1 are located at the center of numerous pathways highlighting their potential functional significance. Western blot analysis confirmed the expression of a subset of the proteins.

Conclusions: Our phosphoproteomic and bioinformatics analysis identified numerous phosphoproteins involved in the regulation of actin dynamics to be differentially expressed in distinct subtypes of T cell lymphoma. Importantly, ALK+ ALCL expressed a distinct signature of actin cytoskeletal phosphoproteins that may be important for the biology of these tumors. Our data reveal the utility of unbiased phosphoteome interrogation of T cell lymphomas in characterizing actin associated signaling networks.

1821 Validation of Targeted Next Generation Sequencing on Ion Torrent Platform for Clinical Testing of Solid Tumors

S Roy, MB Durso, Y Nikiforov, M Nikiforova. University of Pittsburgh, Pittsburgh, PA.

Background: Next generation sequencing technologies have unleashed the possibility of multiplex sequence variation (SV) detection without significant increase in cost. In this study, we evaluated the performance of Ion AmpliSeq™ Cancer Panel on Ion Torrent PGM™ (Life Technologies, San Francisco, CA) for testing of solid tumors in a clinical molecular diagnostic laboratory.

Design: Total of 92 tumors, 8 cell lines and 3 normal tissues were tested for SVs in 46 genes using the Ion AmpliSeq™ Cancer Panel. The validation set included 55 tumors with documented SVs in the *KRAS*, *NRAS*, *HRAS*, *BRAF*, *RET*, *KIT*, *EGFR*, *PDGFR*, *TP53* genes and 37 tumors without SVs. Analysis was performed using the 316 and 318 chips with up to 10 barcoded samples per chip, AmpliSeq v.2.0 chemistry, One Touch 200v2 DL Template kit and Ion PGM Sequencing 200 kit. Data were analyzed using Torrent Suite v2.2, Variant Caller Plugin v2.2.3-31149 and NextGENe® (Softgenetics, State College, PA).

Results: Only 10ng of DNA was sufficient for analysis of all samples (40 frozen, 51 FFPE, 4 FNAs and 8 cell lines) for SVs in 46 genes. An average of 536,660 (189,802–1,334,101) mapped sequence reads per barcoded sample was achieved with the 72bp mean read length, 2,783 mean reads for hot spot coverage, and 92% uniformity of coverage. One hundred percent (53/53) single nucleotide variants, 71% (5/7) deletions and 22% (2/9) insertions were detected with an overall sensitivity of 88%. Manual review of the sequence reads in IGV v.2.1.24 (Broad Institute, Cambridge, MA) revealed 1 deletion and 4 insertion not detected by Variant Caller. In addition to known SVs, novel SVs were detected in the *PIK3CA, TP53, MET, ATM*, and *KDR* genes (confirmed by Sanger sequencing). Multiple low-frequency SVs were detected across all samples and were frequently attributed to read errors in homopolymer regions. A limit of SVs detection was 5-10% depending on coverage depth and turnaround time was 72 hours.

Conclusions: Targeted sequencing using the AmpliSeq™ Cancer panel on Ion Torrent™ PGM allows testing for a broad spectrum of SVs with minimum amount of DNA and rapid turnaround time. Although the sensitivity for detection of single nucleotide variants was 100%, use of alternate protocols is recommended to circumvent the limitations in insertion/deletion detection and homopolymer-associated read errors for clinical use of this platform.

1822 Customized Next Generation Sequencing Tail-End Data Analysis Pipeline for Clinical Cancer Genomics

S Roy, MB Durso, A Wald, Y Nikiforov, M Nikiforova. University of Pittsburgh, Pittsburgh, PA.

Background: Several bioinformatics applications are currently available for processing NGS data. Certain limitations however, preclude the use of such applications in a clinical molecular laboratory. Limited support for 1) customized annotation and platform specific error detection. 2) Customized report generation and ability for cross-talk with existing anatomic pathology laboratory information systems (APLIS) 3) Operating system (OS) commonly used in a clinical laboratory. We attempted to develop a data analysis pipeline to address the above limitations.

Design: TART (Tail-end Analysis and Reporting Tool) is a web-based application developed using ASP.NET version 4.5 (Microsoft, Mountain View, CA). The client-side was scripted using HTML5, CSS3 and JavaScript. The server-side processing relies on interaction with a customized Microsoft SQL server® 2008 R2 (Microsoft, Mountain View, CA) database. This database comprises of three important components – 1) sample and run information 2) Platform specific sequence variation (SV) information and 3) two publically available SV databases; COSMIC (Wellcome Trust Sanger Institute, England) and dbSNP (NCBI). TART is currently designed for processing variant calls generated by targeted next generation sequencing on Ion Torrent PGM.

Results: TART accepts tab-delimited text files, generated by the Variant Caller plugin, as required input. Both variant calls (VC) as well as coverage depth for each hotspot in the mutation panel is processed. Each VC is classified into one of five report levels (1- SV of known clinical significance (CS), 2 – SV of unknown CS, 3 –questionable SV, requiring specific attention, 4 – synonymous SV and 5 – platform specific errors). After pathologist review, the application initiates a "training mode" in response to any change in VC interpretation. As more samples are processed and reviewed by the pathologist, the application "learns" modified or new SV which enriches the database. The report is generated on the server-side in HTML or OpenXML format allowing compatibility with APLIS. The program also allows search and retrieval of archived cases for laboratory quality assurance (QA) activities and research.

Conclusions: This web-based application facilitates rapid and customized VC processing and report generation for targeted next generation sequencing in clinical laboratory. Important advantages include customized annotations, ease of importing reports into APLIS, production of enriched and better annotated SV database, Microsoft Windows OS-support, and report archival and retrieval system.

1823 INDELs in Cancer Detected by Targeted Clinical Next Generation Sequencing

J Sehn, D Spencer, H Abel, E Duncavage. Washington University in St Louis, St. Louis, MO.

Background: The spectrum of insertions and deletions (INDELs) ranging from 1bp to ~1kb is poorly characterized in cancer. Such INDELs can be detected using next generation sequencing (NGS) techniques, with higher resolution than karyotyping, and without prior knowledge of the area of mutation as required for PCR. However, INDEL detection by NGS for targeted oncologic gene panels in routine clinical care remains uncharacterized.

Design: Targeted NGS for 27 cancer genes from 97 consecutive tumor specimens (52 lung, 14 pancreas, 9 colon/rectum, 4 breast, and 18 other) was performed in multiplex using 2x101bp paired-end reads at >1000x coverage. Sequence data were aligned to hg19 and coding region INDELs were identified using Pindel. The accuracy of the INDEL calls was determined by visual inspection of the raw sequence alignments.
Results: Visual review of sequence reads in areas containing INDEL calls revealed that multiple distinct variant annotations were often made by the variant calling software when a single INDEL occurred within a region of low sequence complexity. For these INDELs, the flanking DNA sequences were the same, so the start site of the INDEL was ambiguous, leading to multiple annotations for the same sequence alteration; the end result was an artificially decreased number of supporting reads for each INDEL call. When INDEL calls that by visual inspection represented the same sequence alteration were combined into a single annotation, a total of 292 coding-region INDELs with at least 10 supporting reads were identified (average 5/case, range 0-76/case), 147 of which were insertions and 145 deletions. The average INDEL length was 16 bp (range 1bp-8029bp). Breast carcinomas had the highest average number of INDELs/case (7), followed by colorectal (4), lung (3) and pancreas (2). The most commonly mutation gene was MLL (52).
Conclusions: Targeted NGS of cancer genes shows a constellation of INDELs that are not readily identifiable by other laboratory techniques. Careful review of INDEL calls made by open-source variant calling packages reveals an inherent tendency to annotate a single INDEL with an ambiguous start site as occurring at multiple start sites, with a resulting decrease in the number of supporting reads for each call. Consequently, INDELs with low numbers of supporting reads are filtered out of NGS analyses, contributing to underrepresentation of this potentially clinically relevant class of mutations.

1824 Integrative Genomic Profiling To Identify Drivers of Breast Cancer-Associated Inflammation

MA Seidman, SC Lester, NB Johnson, KH Allison, Y-Y Chen, RE Factor, GMK Tse, SJ Shin, DA Eberhard, PH Tan, SJ Schnitt, LC Collins, KC Jensen, K Korski, FM Waldman, AH Beck. Cancer Genome Atlas (TCGA) Breast Cancer Expert Pathology Committee, Bethesda, MD.
Background: Host immune response to tumors is variable between individuals and is a strong prognostic factor in breast cancer, with increased lymphocytic inflammation associated with improved prognosis. The tumor genomic determinants of host inflammation are not well understood.
Design: To determine genomic factors associated with the inflammatory response in breast cancer, we assembled a Breast Cancer Expert Pathology Committee to score inflammation on digital whole slide images of breast cancer specimens undergoing molecular profiling as part of The Cancer Genome Atlas project. Inflammation was scored as either present or insignificant/absent on 281 cases. We analyzed genome-wide DNA copy number variation data (both normalized log2 ratio values and GISTIC-processed copy number calls) and expression profiling data (acquired both by microarray and by RNAseq) to identify genes that were significantly associated (positively or negatively) with inflammation by both DNA copy number and RNA expression, and thus restricted to tumor cells. This analysis was implemented by performing a series of two-class SAM analyses and identifying genes significantly associated, either positively (inducers) or negatively (repressors), with inflammation in all of the analyses.
Results: This analysis identified 1271 genes significantly associated with host inflammation by both RNA expression and DNA copy number in all analyses at a false discovery rate threshold of 5%. We performed gene set enrichment analysis of this gene signature, including 1081 genes where DNA copy number gain and over-expression is associated with increased inflammation (i.e. inducers) and 190 genes where DNA copy number loss and under-expression are associated with increased inflammation (i.e. repressors). The gene-set is significantly enriched for pathways related to cell cycle regulation, transcription, and DNA repair, pathways related to breast cancer pathogenesis, and pathways relating to leukocyte migration and T-cell function. Additionally, several drug associated gene signatures were identified as enriched in the inflammation-associated genomic signature. These include a subset of down-regulated genes also reportedly down-regulated by specific HDAC1 inhibitors, suggesting a possible adjuvant therapeutic for breast cancer.
Conclusions: This integrative analysis of breast cancer genomic data and host inflammatory response provides insights into the biology of tumor associated inflammation as well as identifies candidates for new therapeutic approaches to modulate host inflammatory response to breast cancer.

1825 PIK3CA Mutations Are Common in Many Tumor Types and Are Often Associated with Other Concurrent Mutations

MD Stachler, N Lindeman. Brigham and Women's Hospital, Boston, MA.
Background: PIK3CA mutations have been commonly reported in a variety of cancers. The widespread nature of PIK3CA mutations has generated significant interest in developing targeted therapy. Unfortunately, to date there has been limited success with these therapeutics. Many of the patients enrolled in these trials have had limited, if any, molecular testing. Tumor genotyping clinical cancer specimens provides an opportunity to determine a fuller spectrum of mutations an individual tumor harbors and thus provide better insight into its molecular pathogenesis. Using this data may improve the design, rationale, and outcome of PI3K targeted therapy.
Design: Invasive cancer samples of all types containing >250 ng of DNA were genotyped for 471 mutations in 41 cancer-associated genes (including 15 mutations in PIK3CA) using a PCR-mass spectrometry assay (Sequenom). The number of PIK3CA mutations found from each primary tumor site was quantified. The total number and types of mutations each sample harbored was compared between PIK3CA mutated and non-PIK3CA mutated samples.
Results: A total of 1973 cancers were genotyped. 172(9%) contained a mutation in PIK3CA, involving 22 different primary sites. Most PIK3CA mutation frequencies were similar to what has been reported by the Sanger Center (COSMIC), however a significantly higher prevalence was observed in cancers of the endometrium, biliary tract, and liver and a lower prevalence was seen in cutaneous cancers. Interestingly, in 79(45%) cases the PIK3CA mutation was found with at least one other mutation while only 6% of the non PIK3CA mutated cases had more than one mutation ($p<0.0001$). The additional mutations found with PIK3CA tended to be in the Ras/Raf pathway, WNT pathway, or in growth factor receptors, but were varied.
Conclusions: PIK3CA mutations are found in a wide variety of tumors and tend to occur with other mutations. This suggests that either PIK3CA mutations are a late event (possibly evan a "passenger" mutation) or lead to additional mutations. Previous studies have shown PIK3CA mutations to be associated with advanced disease in several cancers. These findings also have implications for targeted therapy. If other pro-oncogenic pathways are commonly mutated along with PIK3CA, then PIK3CA inhibition alone may not be effective and combination therapy may be warranted.

1826 The Proportion of Contaminating Host Organ RNA within Clinical Biopsies of Metastatic Breast Cancer Is Minimal

H Sun, C Hatzis, C Fu, R Avritscher, K Ahrar, A Tam, S Curley, H Yao, J-N Vauthey, V Valero, D Booser, D Maru, S Hamilton, R Luthra, R Lau, RE Gould, L Pusztai, M Wallace, WF Symmans. MD Anderson Cancer Center, Houston, TX; Nuvera Biosciences, Woburn, WA.
Background: Host organ contamination is a limitation for DNA-based testing of small biopsies from metastatic sites that is currently addressed by histologic assessment of tumor cellularity and/or microdissection. Relatively higher transcriptional activity in tumor cells might favor RNA-based testing. Therefore, we used breast cancer within liver as a model to predict the extent of host organ RNA contamination in gene expression microarrays of radiologically-guided clinical biopsies from liver metastases of breast cancer.
Design: Microarray-based (Affymetrix U133A, Santa Cruz, CA) multi-gene expression indices were developed to measure genes that either *discriminate* normal liver from breast cancer or have expression levels that *calibrate* to the proportion of liver RNA spiked into breast cancer RNA. These discriminating and calibrating multi-gene liver indices, and the reverse transcription-polymerase chain reaction (RT-PCR) measurements of a single discriminating liver gene (*CYP2E1*) were tested in a blinded validation study cohort of 30 known mixtures of breast cancer and liver RNA. Finally, the proportion of liver RNA contamination was estimated in clinical liver biopsies from 23 patients with metastatic breast cancer.
Results: The correlation coefficient for concordance (CCC) between predicted and actual percent liver RNA in the blinded validation study was higher for the RT-PCR assay for *CYP2E1* (0.894) than for the discriminating 16-gene index (0.679) or the calibrating 10-gene index (0.663) measured from microarrays. All three assays slightly overestimated the percent liver RNA in a mixture. Of 23 clinical biopsies, the better microarray-based predictor (calibrating index) predicted <5% liver RNA in 13/23, <10% in 16/23, and <20% in 21/23. Of 17 biopsies with sufficient remaining RNA, the RT-PCR assay predicted <1% liver RNA in 10/17, <5% liver RNA in 16/17, and 12.6% liver RNA in one case.
Conclusions: It is likely that the majority of radiologically-guided clinical biopsies of metastatic breast cancer in the liver contain >90% breast cancer RNA. This was bested estimated using an RT-PCR assay that could become a quality control procedure. The relatively low proportion of contaminating host organ RNA might offer an advantage to RNA-based, rather than DNA-based, genomic tests of metastatic samples.

1827 Desktop Transcriptome Sequencing from Archival Tissue To Identify Clinically Relevant Translocations

RT Sweeney, B Zhang, SX Zhu, S Varma, K Smith, SB Montgomery, M van de Rijn, J Zehnder, RB West. Stanford School of Medicine, Stanford, CA.
Background: Somatic mutations, often translocations or single nucleotide variations, are pathognomonic for certain types of cancers and are increasingly of clinical importance for diagnosis and prediction of response to therapy. Conventional clinical assays only evaluate one mutation at a time and targeted tests are often constrained to identify only the most common mutations. Genome-wide or transcriptome-wide high throughput sequencing (HTS) of clinical samples offers an opportunity to evaluate for all clinically significant mutations with a single test. Recently "desktop versions" of HTS have become available, but most of the experience to date is based on data obtained from high quality DNA from frozen specimens. In this study, we demonstrate, as a proof of principle, that translocations in sarcomas can be diagnosed from formalin fixed paraffin embedded (FFPE) tissue with desktop HTS.
Design: Using a first-generation desktop sequencer, full transcriptome sequencing was performed on FFPE material from archival blocks of 3 synovial sarcomas, 3 myxoid liposarcomas, 2 Ewing's sarcomas, and 1 clear cell sarcoma. All of the chosen cases were less than six months old and had their respective pathognomonic translocations confirmed by FISH. The reads were mapped to the "sarcomatome" (all currently known 83 genes involved in translocations and mutations in sarcoma) and a novel algorithm was developed for ranking fusion candidates.
Results: The pathognomonic fusions and the exact breakpoints were identified in all cases of synovial sarcoma, myxoid liposarcoma, and clear cell sarcoma. The Ewing sarcoma fusion gene was detectable in FFPE material only with a sequencing platform that generates greater sequencing depth.
Conclusions: The results show that a single transcriptome HTS assay, from FFPE, has the potential to replace conventional molecular diagnostic techniques for the evaluation clinically relevant mutations in cancer.

1828 Genetic Heterogeneity of Gleason Score 7 Prostate Cancer: A Pilot Study of the Canadian Prostate Cancer Genome Network (CPC-GENE)

D Trudel, M Fraser, ER Lalonde, A Meng, A Brown, T Chong, A Zia, M Sam, PH Hennings-Yeomans, F Yousif, R Denroche, J Johns, L Timms, N Buchner, R de Borja, NJ Harding, MA Chan-Seng-Yue, J Wang, G Zafarana, MHW Starmans, M Pintilie, N Fleshner, S Volik, L Muthuswamy, C Collins, TJ Hudson, LD Stein, T Beck, JD McPherson, T van der Kwast, PC Boutros, RG Bristow. University of Toronto, Toronto, Canada; University of British Columbia, Vancouver, Canada.

Background: Despite the use of Gleason score as the most important prognostic factor in prostate cancer (CaP), our genetic studies using aCGH have shown that tumors with the same Gleason score can vary 100 fold in genetic instability. Furthermore, CaP is a multifocal and, likely, a multi-clonal disease as reflected in part by the heterogeneity in TMPRSS2:ERG fusion status in different tumor foci from a single prostate. In the era of personalized medicine, there is an urgent need to characterize inter- and intra-prostate molecular heterogeneity for patient stratification.

Design: The Canadian Prostate Cancer Genome Network (CPC-GENE) has undertaken a pilot study to provide an evaluation of the heterogeneity in Gleason score 7 PCa using a robust genomic approach. Gleason score (GS) 4+3 and 3+4 tumors from 5 frozen radical prostatectomies were analyzed using whole-genome sequencing (WGS) and Affymetrix OncoScan SNP arrays to determine differential genetic signatures. DNA from formalin-fixed, paraffin-embedded (FFPE) foci from the prostatectomies was analyzed by WGS after tumor mapping according to histopathology characteristics, including ERG immunostaining. Tumor foci were manually macrodissected before DNA extraction. For each patient, germline DNA from whole blood was used as a control.

Results: A total of 28 tumor foci from 5 prostates were sequenced (frozen: 5; FFPE: 18). Across multiple specimens, single nucleotide variants (SNVs) and copy number variations (CNVs) identified using WGS were validated with ~98% accuracy against the OncoScan platform. Analysis of germline SNV profiles suggests a concordance of ~99% between tumor regions (~3.7 million germline SNVs/patient). A median of 55 somatic SNVs were identified in the 28 foci (interquartile range: 36-75) and nearly all SNVs were unique to a tumor focus. CNV profiles were heterogeneous among the cases. In two cases with > 4 sequenced foci, CNVs segregated according to localization in the prostate. In one case with 4 ERG-positive and 4 ERG-negative foci, the SNV profiles of the foci segregated according to ERG status. Sub-clonal phylogenetic analyses revealed evidence of independent tumor origins in at least one case.

Conclusions: The number of identified variants suggests a high degree of intra-focal and intra-prostatic genetic heterogeneity in GS7 PCa, and we brought further information about PCa intraprostatic phylogeny. This could be important both in the identification of the significant tumor focus and in the capacity to act on targetable mutations.

1829 Structural and Functional High-Throughput Genome Analysis Helps Differential Diagnosis between Follicular Adenomas and Carcinomas: Results in a Series of 62 Patients

P Vielh, C Richon, G Meurice, B Job, Z Balogh, A Valent, L Lacroix, V Marty, N Motte, P Dessen, B Caillou, A Al Ghuzlan, J-M Bidart, V Lazar, AK El-Naggar, M Schlumberger. Institut Gustave Roussy, Villejuif, France; MD Anderson Cancer Center, Houston, TX.

Background: Although fine needle aspiration (FNA) cytology is an efficient method for diagnosing the benign or malignant nature of thyroid nodules, distinction between follicular adenomas (FA) and follicular carcinomas (FC) may still represent a difficult task. Identification of distinct structural and functional genomic alterations between these two groups of tumors, potentially applicable to cytological specimens, would be therefore of major interest. Our previous array comparative genomic hybridization (aCGH) results showed that by testing 3 chromosomal abnormalities 50% of the carcinomas can be identified (USCAP 2011, [1208]). In this study, genomic aberrations detected by fluorescent *in situ* hybridization (FISH) and transcriptomic profile assessed by microarray are studied in a series of frozen samples from histologically proven FA and FC.

Design: A large set of molecular abnormalities in a cohort of 62 patients (see table) were analyzed by molecular methods. All samples underwent FISH analysis using commercially available probes specific to the 3 already described chromosomal anomalies on touch preparations of the corresponding tumors to define aberrant status. Samples with good RNA quality were further hybridized on Agilent 8x60K microarrays (AMADID 28004) to obtain their transcriptomic profile.

The cohort of follicular carcinomas (FC) and follicular adenomas (FA) of the thyroid.

Chromosomal Abnormalities Detected*	FC**	FA**	Total**
Yes	18 (13)	0 (0)	18 (13)
No	18 (10)	26 (17)	44 (27)
Total	36 (23)	26 (17)	62 (40)

*Chromosomal abnormalities were tested by FISH. **The number of samples on which gene expression profiling were performed is in brackets.

Results: The class comparison of transcriptomic profile between FA and FC not having chromosomal abnormalities raised a list of 242 transcripts. These transcripts classified all of the profiles in two groups: one composed of 13 adenomas, the other composed of 10 carcinomas and 4 adenomas known to be mutated in either *KRAS*, *HRAS* or *NRAS* genes (data not shown).

Conclusions: In the group of follicular lesions without chromosome alteration detected by FISH, gene expression profiling is able to further differentiate adenomas from carcinomas. These preliminary results should now be validated on an independent series.

1830 Expression Profiling and Molecular Classification of Colorectal Cancer: Meta-Analysis of 8 Independent mRNA Expression Datasets across the Globe

L Waldron, G Parmigiani, C Fuchs, C Huttenhower, S Ogino. Dana-Farber Cancer Institute, Boston, MA; Harvard School of Public Health, Boston, MA; Brigham and Women's Hospital, Harvard Medical School, Boston, MA.

Background: Gene expression profiling has not reproducibly sub-classified colorectal cancers. In addition to the existing tumor biomarkers such as KRAS, BRAF, and MSI, gene expression profiling may provide clinically useful classification system, as well as biological insights.

Design: We meta-analyzed 8 genome-wide mRNA expression datasets (total N=2001). We performed gene expression profiling of 718 cases of archival colorectal cancer tumors, using the Illumina DASL microarray platform. We performed strict quality control for both samples and gene probes. We also obtained data from 7 independent studies on transcirptomic profiling from publicly available database; a total of 1,283 samples from fresh-frozen tissues. These 2,001 samples formed a basis for identifying and validating discrete or continuous subtypes present across research centers and study populations.

Figure 1 (Table). Datasets available for meta-analysis

Citation	Accession ID	# features after variance filter	# samples	Microarray platform
Jorissen 2008	GSE13294	8156	155	Affymetrix HG-U133_Plus_2
Watanabe 2011	GSE14095	18663	189	Affymetrix HG-U133_Plus_2
Jorissen 2009	GSE14333	5048	290	Affymetrix HG-U133_Plus_2
Smith 2010	GSE17536	440	177	Affymetrix HG-U133_Plus_2
Kogo 2011	GSE21815	7464	141	Agilent-014850
Sanz-Pamplona 2011	GSE26682-GPL570	764	176	Affymetrix HG-U133_Plus_2
Sanz-Pamplona 2011	GSE26682-GPL96	560	155	Affymetrix HG-U133A
Current data	GSE32651*	2069	718	Illumina WG-DASL v3

Results: We identified reproducible expression profiling clusters by principal component analysis (PCA). In addition, we were able to validate MSI-high-associated signatures across studies. Notably, gene set enrichment analysis (GSEA) showed that a number of immunity-related pathways represented reproducible signatures, which differentiated subtypes of colorectal cancers across the studies.

Figure 2. Gene Set Enrichment Analysis (GSEA) results

	Number of genes	p-value	Bonferroni correction
BIOCARTA_TCRA_PATHWAY	11	1.83E-06	0.000397
BIOCARTA_TCYTOTOXIC_PATHWAY	10	6.08E-06	0.001319
BIOCARTA_THELPER_PATHWAY	10	6.73E-06	0.00146
BIOCARTA_IL17_PATHWAY	12	3.44E-05	0.007463
BIOCARTA_INFLAM_PATHWAY	12	4.07E-05	0.008839
BIOCARTA_CSK_PATHWAY	20	0.000127	0.027629
BIOCARTA_CTL_PATHWAY	12	0.000161	0.034845
BIOCARTA_GRANULOCYTES_PATHWAY	9	0.000417	0.090497
BIOCARTA_LYM_PATHWAY	8	0.000718	0.155855
BIOCARTA_CYTOKINE_PATHWAY	5	0.0008	0.173557
BIOCARTA_LAIR_PATHWAY	14	0.000914	0.198334
BIOCARTA_TCAPOPTOSIS_PATHWAY	7	0.000924	0.200563
BIOCARTA_STATHMIN_PATHWAY	16	0.001136	0.246529
BIOCARTA_IL5_PATHWAY	7	0.001561	0.338755
BIOCARTA_CTLA4_PATHWAY	17	0.001594	0.34594
BIOCARTA_DC_PATHWAY	9	0.003584	0.777817
BIOCARTA_MCM_PATHWAY	11	0.004284	0.929714
BIOCARTA_TCR_PATHWAY	36	0.004506	0.977788
BIOCARTA_RELA_PATHWAY	10	0.999477	1

Conclusions: Genome-wide mRNA expression data can provide useful information in colorectal cancer molecular classification. In particular, MSI-high is associated with reproducible differentially up-regulated and down-regulated genes. Our data support that immunity-related pathways are important in colorectal tumor biology, reflecting the fact that tumor consists of both transformed epithelial cells and non-neoplastic stromal and immune cells, all of which interact in the tumor microenvironment.

1831 miRNA Profiling by Next Generation Sequencing and miRNA ISH in Ulcerative Colitis Neoplastic Progression

NC Welker, J Lin, MP Bronner. ARUP Institute for Clinical and Experimental Pathology, Salt Lake City, UT; University of Indiana, Indianapolis, IN; University of Utah, Salt Lake City, UT.

Background: Ulcerative colitis (UC) represents a classic chronic inflammatory disease model linked to neoplastic progression. While the lifetime risk of colon cancer is only ~10% in UC, no effective means currently exist to distinguish this subset. Prior UC studies reveal widespread colonic mucosal molecular alterations that extend far beyond histologic dysplasia to even involve nondysplastic rectal mucosa. Improved bioclassifiers that build on this knowledge in UC are highly sought after to better identify the subset

of patients most likely to benefit from expensive and difficult surveillance procedures.
Design: Non-dysplastic rectal biopsies were analyzed from 10 UC patients with synchronous but distant colon cancer (UC-progressors), 10 without dysplasia for >10 years (UC-nonprogressors), and 18 normal controls. Next generation small RNA sequencing was performed on the Illumina platform. Data were analyzed using the USeq software package to determine regions of differential expression between these patient groups. RT-PCR, in situ hybridization, and immunohistochemistry were performed for validation purposes and to identify which cells differentially express micro-RNAs within the tested biopsies.
Results: While 11 miRNAs were misregulated in both UC patient groups compared to normals, a total of 33 miRNAs were differentially expressed between progressors and nonprogressors using our statistical criteria (fold change >2, false discovery rate < 0.10). RT-PCR confirmed these RNA-sequencing results. Of particular interest, mir-155 was overexpressed in UC-nonprogressors, but not UC-progressors. Mir-155 has been implicated in the regulation of T-cell subsets, particularly Th17 cells that express IL-17. In situ hybridization using a mir-155 specific probe and IHC staining for IL-17 validate these biomarkers in situ within lamina propria lymphocytes.
Conclusions: We have identified a subset of miRNAs that are specifically misregulated in UC-nonprogressor and progressors that may prove useful as a biomarker panel to enhance early cancer detection and prevention in UC. Mir-155 is implicated in controlling the immune cell environment in UC. Its involvement as a biomarker has been validated by RT-PCR, in situ hybridization and immunohistochemistry for TH17 cells in nondysplastic rectal biopsies.

1832 Mutation Profiling of Bladder Cancer Using Ion Torrent Sequencing

EM Wojcik, AB Rosenfeld, MI Zillox, ML Quek, GA Barkan, X Gai. Loyola University, Maywood, IL.
Background: Urothelial carcinoma of the bladder (UC) is the second most common genitourinary malignancy in the United States. Current diagnostic tests are based on a specific biomarker or genetic alteration, and have modest sensitivity and specificity. We hypothesize that mutation profiles of known oncogenes and tumor suppressor genes collectively can distinguish different subgroups, therefore be used for accurate diagnosis, prognostic monitoring, and predicting treatment response.
Design: Histopathological examination of formalin-fixed, paraffin-embedded (FFPE) samples differentiated normal bladder tissue from tumor tissue (High grade UC, T2b). In a pilot study, DNA was isolated from pairs of UC and normal tissues of 5 patients using the AMBION Recovery all protocol. Genomic regions encompassing 739 known COSMIC mutations in 46 oncogene and tumor suppressor genes were amplified using Ion Torrent Ampliseq cancer panel protocol, which were then sequenced using the Ion Torrent Personal Genome Machine. An average base coverage depth of 570X across all target regions was achieved. Variant calls were made using the Ion Torrent Suite of software tools.
Results: We detected 7-40 genetic variants in each sample, with the majority being previously unknown somatic mutations. The overlap between the normal and cancerous tissue was less than 30% in each patient, suggesting the histologically normal tissues were possibly pre-cancerous. We found variants in exons, introns and the 3' UTR of genes that resulted in 52 silent, 83 missense and 5 nonsense coding changes. In addition, we detected 9 deletions resulting in frameshifts. Further analysis using this limited sample size suggested a positive correlation of the number of mutations with patient age. Between patients, we found the highest number of mutations in the APC, FGFR3, KDR and PDGFRA genes with few overlaps.
Conclusions: Our results revealed a large number of novel cancer mutations and confirmed 1) the highly heterogeneous nature of urothelial carcinoma, both within and between samples, 2) the presence of a large number of somatic mutations in the histologically normal surrounding tissues; 3) the lack of a common bladder cancer mutation in these oncogenes and tumor suppressor genes, and hence 4) the potential need of personalized genetic test for each patient. In addition, our preliminary results are in agreement with the hypothesis that accumulation of somatic mutations in the bladder cells as people age leads to pre-cancerous cells and eventually cancer.

1833 Whole Genome Analyses of Pancreatic Acinar Cell Carcinomas

LD Wood, Y Jiao, R Yonescu, JA Offerhaus, DS Klimstra, A Maitra, N Papadopoulos, KW Kinzler, B Vogelstein, RH Hruban. Johns Hopkins University, Baltimore, MD; University Medical Center Utrecht, Utrecht, Netherlands; Memorial Sloan-Kettering Cancer Center, New York, NY.
Background: Acinar cell carcinoma, a rare pancreatic carcinoma, is morphologically distinct from other pancreatic neoplasms, with unique clinical and immunohistochemical features. However, the genetic alterations underlying the development of acinar cell carcinoma have not yet been systematically explored.
Design: Twenty-three fresh frozen acinar cell carcinomas were macrodissected to achieve a neoplastic cellularity of >70%. Whole exome sequencing was performed on each carcinoma and matched normal tissue using next generation sequencing technology. The data were filtered for quality, and the alterations in the matched tumor and normal tissues were compared to identify tumor-specific somatic mutations. In addition, copy number arrays were performed on each tumor to identify large genomic alterations.
Results: Acinar cell carcinomas were characterized by striking genomic instability. While some carcinomas exhibited microsatellite instability, as evidenced by enrichment for single-base substitution mutations, other carcinomas showed marked chromosomal instability, with numerous large gains and losses throughout the genome. Chromosomal instability was validated by FISH which highlighted dramatic chromosomal alterations. Sequencing also revealed numerous somatic mutations. Acinar cell carcinomas contained somatic mutations in multiple components of the WNT signaling pathway (including *APC* and *CTNNB1*). Somatic mutations were also identified in druggable targets, including multiple hotspot mutations in *BRAF*. Infrequent somatic mutations were identified in genes known to be involved in pancreatic ductal adenocarcinoma, such as *TP53* and *SMAD4*, as well as genes involved in cystic neoplasms of the pancreas, such as *GNAS*. Acinar cell carcinomas lacked mutations in other genes implicated in pancreatic neoplasia, including *KRAS* and *ATRX/DAXX* (seen in pancreatic neuroendocrine tumors). In addition, acinar cell carcinomas contained somatic mutations in many genes not previously implicated in pancreatic neoplasia, indicating that these neoplasms are genetically distinct from the other neoplasms in the pancreas.
Conclusions: High-throughput molecular analyses of acinar cell carcinomas revealed that these carcinomas exhibit striking genomic instability. Although these carcinomas contain some genetic overlap with other pancreatic neoplasms, the results of this study indicate that acinar cell carcinomas are a genetically distinct neoplasm, possibly explaining their unique clinical behavior.

Pathobiology

1834 Detection of PML/RARA Fusion Protein in APL Using Proximity Ligation Assay as an Alternative to FISH Testing

J Bodo, JJ Lin, JP Maciejewski, AE Schade, ED Hsi. Institute of Pathology and Laboratory Medicine, Cleveland Clinic, Cleveland, OH; Taussig Cancer Institute, Cleveland Clinic, Cleveland, OH; Diagnostics Research/Development, Eli Lilly and Company, Indianapolis, IN.
Background: The presence of t(15,17)(q22;q12) resulting in *PML/RARA* fusion in acute promyeolocytic leukemia (APL) causes determines eligibility for immediate specific therapy. Currently, FISH and qPCR may be used to distinguish APL from other types of AML. We have developed a brightfield, slide-based method for the rapid *in situ* detection of the PML/RARA fusion protein using proximity ligation assay (PLA) and evaluated the correlation between PML/RARA fusion protein expression in APL and *PML/RARA* rearrangement.
Design: A total of 10 AML and APL cytospin samples with known *PML/RARA* FISH status were stained using PLA (OLINK Bioscience, Uppsala, Sweden) with PML and RARA specific antibodies. The principle of PLA is the recognition of target by two antibodies that can bring into proximity oligonucleotides that are conjugated to secondary antibodies. The oligos participate in ligation, creating a template for generating a large, tethered DNA molecule by amplification and detected with labeled hybridization probes, followed by brightfield detection.
Results: PLA was optimized with the NB-4 cell line (APL cell line with PML/RARA fusion protein) and SU-DHL-6 cell line (DLBCL cell line lacking PML/RARA fusion protein, but expressing normal PML and RARA). All 5 *PML/RARA* FISH positive APL cases were positive for PML/RARA expression by PLA. The majority of tumors cells were positive in *PML/RARA* rearranged cases (Figure 1). Importantly, there was no false positive staining among the 5 AML cases lacking t(15;17).
Conclusions: Early detection of PML/RARA is critical for directing appropriate therapy in APL. Our PLA specifically identified *PML/RARA*+ APL cases and can be performed and analyzed without specialized equipment. This is proof of principle that PLA can be used to detect clinically relevant fusion proteins with brightfield microscopy within a few hours.

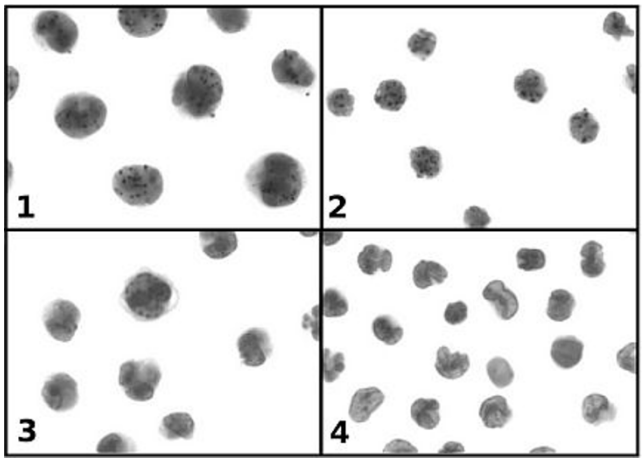

Figure 1. Detection of PML/RARA fusion protein expression by PLA. NB-4 (1) and SU-DHL-6 (3) cells served as positive and negative controls, respectively. Examples of PML/RARA+ APL (2) and PML/RARA- AML (4) samples are shown.

1835 Progesterone Induces NF-kB Activation through PI3K/Akt-2 Signal Pathway Which Regulates Focal Adhesion Kinase (FAK) in MCF-7 Breast Cancer

F Candanedo-Gonzalez, R Espinosa-Neira, S Villegas-Comonfort, N Serna Marquez, P Cortes-Reynosa, E Perez Salazar. Oncology Hospital, National Medical Center Century XXI, IMSS, Mexico City, Mexico; CINVESTAV-IPN, Mexico City, Mexico.
Background: Around 75% of breast tumors are positive for the progesterone receptor (PR). However, the signal transduction pathways activated by progesterone have not been studied in detail. The phosphatidyl inositol 3-kinase (PI3K) pathway plays an important role in breast cancer progression. Downstream of PI3K, Akt1 and Akt2, have opposing roles in breast cancer invasion migration, which lead to metastatic